

Phase diagram of the one-dimensional t_1 - t_2 - J model: Ferromagnetism, triplet pairing, and charge and pair density waves

Luhang Yang^{1,*} and Adrian E. Feiguin^{2,†}

¹Stanford Institute for Materials and Energy Sciences, SLAC National Accelerator Laboratory, Menlo Park, California 94025, USA

²Department of Physics, Northeastern University, Boston, Massachusetts 02115, USA



(Received 12 March 2024; revised 28 May 2024; accepted 18 June 2024; published 9 August 2024; corrected 2 October 2024)

We present a density matrix renormalization group study of an extended t - J model with hopping to the first and second neighbors—the one-dimensional t_1 - t_2 - J model. The full phase diagram as a function of the density n and exchange strength J , for both positive and negative values of t_2 , is obtained. For $t_2 = -0.5$ we observe that, in the strongly interacting region, Nagaoka ferromagnetism is accompanied by a triplet pair density wave (PDW) upon doping. As the spin exchange J increases, a charge density wave phase emerges and then gives way to singlet superconductivity (SC). This phase behaves as a singlet PDW with vanishing spacial average of the order parameter and a spin gap. When $t_2 = 0.5$, the physics is basically reminiscent of the conventional t - J model, undergoing a transition from a metallic to a SC phase as a function of J .

DOI: [10.1103/PhysRevB.110.085122](https://doi.org/10.1103/PhysRevB.110.085122)

I. INTRODUCTION

The role of particle-hole asymmetry in high-temperature superconductors [1–7] has been a long-time puzzle. Some properties in the low-energy regime can be reproduced by Hubbard-like models and there is evidence pointing toward doped cuprates possibly being described by an effective t_1 - t_2 - J model with the hole (electron) asymmetry accounted for by a second-neighbor hopping [6,8–16]. In the t_1 - t_2 Hubbard model, a particle-hole transformation changes the sign of t_2 and maps the upper Hubbard band into the lower Hubbard band. The t_1 - t_2 - J model in its original formulation can only represent a hole-doped Mott insulator. However, it can be interpreted as representing the electron-doped side after flipping the sign of t_2 . Theoretical studies on these microscopic models reveal that on the electron-doped side, the effect of second-neighbor hopping is to enhance superconductivity, while the superconducting order is suppressed in a large region on the hole-doped side [17–19]. This discrepancy between theory and experiment has not been fully resolved. Although most of the numerical evidence suggests that hole doping does not favor superconductivity, recent state-of-the-art large-scale numerical studies of the t_1 - t_2 - J model on six and eight-leg cylinders indicate the emergence of the d -wave SC [20–22].

Many questions remain that still do not have a satisfactory answer, such as whether stripes or charge density waves are coexisting or competing with superconductivity [23–33] or determining the role of antiferromagnetic (AFM) fluctuations in cuprate superconductors [34]. A recent study of an extended t - J model on wide cylinders (ladders of six to eight legs) shows that AFM and singlet d -wave SC orders coexist at low electron doping, while in the hole-doped regime the stripe

order suppresses superconductivity [19]. Relevant studies on the two-dimensional (2D) square lattice also suggests that on the electron-doped side, AFM order is stabilized near half filling but is absent on the hole-doped side [10].

In order to tackle these questions, a systematic study of the phase diagram in the entire doping range for the one-dimensional t_1 - t_2 - J model may shed some light on the possible instabilities of the model in higher dimensions. As a recent example, the one-dimensional cuprate $\text{Ba}_{2-x}\text{Sr}_x\text{CuO}_{3+\delta}$ exhibits spectral features that cannot be simply explained by means of the one-band Hubbard model [35,36].

While two-dimensional calculations for the whole doping range are still not accessible by any numerical method, the study of one-dimensional and quasi-one-dimensional systems can be informative about the interplay between intertwined and competing orders and their doping dependence. By introducing the second-neighbor hopping, the single-particle electronic band structure will be changed and, in the one-dimensional case, it also changes the coupling between the spin and charge channels [37,38].

The model realizes interesting physics in both high- and low-doping regimes [37,39,40]. Most studies have been focused on the ferromagnetic (FM) phase in the small- J limit (or large U in the Hubbard model) [41–43]. The possibility of ferromagnetism in the Hubbard model was first proposed by Nagaoka [44] in the limit of infinitely strong on-site Coulomb interactions in two spatial dimensions. By introducing a negative second-neighbor hopping, Nagaoka’s FM can be extended to the 1D Hubbard model [45]. Numerical studies have shown that for a finite value of U_{critical} , the FM transition happens at a smaller electron density when increasing $|t_2|$ [46]; this means that both the “single hole doping” and “infinite U ” conditions for Nagaoka FM can be relaxed. The t_1 - t_2 - U model with $t_2 < -t_1/4$ is one of the few models that have been found to have a fully polarized FM ground state [47,48]. Furthermore, the existence of FM states opens the possibility of

*Contact author: luhyang@stanford.edu

†Contact author: a.feiguin@northeastern.edu

triplet superconductivity [49–51]. However a comprehensive understanding and a full phase diagram in the whole range of doping densities is still missing.

The main findings of this study are as follows: (i) for $t_2/t_1 = -0.5$ we observe an FM metallic phase accompanied by a triplet-SC order when J is small and a CDW phase when J is of the order of t_1 , giving way to a superconducting phase with pair density wave character by increasing J ; (ii) when $t_2/t_1 = 0.5$, we find a phase diagram qualitatively similar to the one of the conventional t - J model. At large-enough J , we always encounter phase separation.

The paper is organized as follows: In Sec. II, we introduce the model Hamiltonian and the method used in this work; in Sec. III we present the phase diagram for $t_2/t_1 = \pm 0.5$, followed by a systematic study of the ground-state properties in the different phases. We close with a discussion of our findings.

II. MODEL AND METHODS

The t_1 - t_2 - J model we study in this work is written as:

$$H_{t_1-t_2-J} = - \sum_{i,j,\sigma} t_{ij} (c_{i,\sigma}^\dagger c_{j,\sigma} + \text{H.c.}) + J \sum_i \left(\vec{S}_i \cdot \vec{S}_{i+1} - \frac{1}{4} n_i n_{i+1} \right), \quad (1)$$

where $c_{i\sigma}^\dagger$ is the electron creation operator on site i with spin index $\sigma = \uparrow, \downarrow$, n_i is the electron number operator, and \vec{S}_i is the spin $S = 1/2$ operator on site i . We set the first-neighbor hopping $t_{ij} = t_1 = 1$ as our unit of energy, $t_{ij} = t_2$ when i, j are next nearest neighbors, and zero otherwise. Double occupancy is implicitly prohibited.

In order to determine the phase diagram and ground-state properties, we study the problem numerically using the DMRG method [52,53] for two system sizes: $L = 64$ and $L = 96$. By keeping the bond dimension $m = 1600$, we make sure that the truncation error remains below 10^{-7} . We compute several correlation functions to characterize the ground-state properties and determine the phase diagram. The spin-spin correlations are given by:

$$S(r) = \langle S_0^z S_r^z \rangle; \quad (2)$$

the density-density correlations as:

$$D(r) = \langle n_0 n_r \rangle - \langle n_0 \rangle \langle n_r \rangle; \quad (3)$$

the single-particle correlations as:

$$G(r) = \langle c_{0,\uparrow}^\dagger c_{r,\uparrow} \rangle; \quad (4)$$

and the local density distribution as:

$$N(r) = \langle c_{r,\uparrow}^\dagger c_{r,\uparrow} + c_{r,\downarrow}^\dagger c_{r,\downarrow} \rangle. \quad (5)$$

Pairing instabilities will be determined by calculating the singlet pair-pair correlations:

$$P_s(r) = \langle \Delta_0^\dagger \Delta_r \rangle, \quad (6)$$

where Δ^\dagger operator creates a singlet pair on neighboring sites,

$$\Delta_i^\dagger = \frac{1}{\sqrt{2}} (c_{i,\downarrow}^\dagger c_{i+1,\uparrow}^\dagger - c_{i,\uparrow}^\dagger c_{i+1,\downarrow}^\dagger). \quad (7)$$

We also introduce the triplet pair-pair correlations:

$$P_t(r) = \langle \tilde{\Delta}_0^\dagger \tilde{\Delta}_r \rangle + \langle c_{0,\downarrow}^\dagger c_{1,\downarrow}^\dagger c_{r,\downarrow} c_{r+1,\downarrow} \rangle + \langle c_{0,\uparrow}^\dagger c_{1,\uparrow}^\dagger c_{r,\uparrow} c_{r+1,\uparrow} \rangle, \quad (8)$$

where $\tilde{\Delta}^\dagger$ operator creates a triplet pair on neighboring sites:

$$\tilde{\Delta}_i^\dagger = \frac{1}{\sqrt{2}} (c_{i,\downarrow}^\dagger c_{i+1,\uparrow}^\dagger + c_{i,\uparrow}^\dagger c_{i+1,\downarrow}^\dagger). \quad (9)$$

These correlations are computed to characterize each phase and establish the dominant order. Notice that in one dimension, their behavior can only be algebraic, or exponential with distance. For instance, in the CDW phase one finds a sharp peak in the density structure factor at the ordering wave vector, and the density-density correlation dominates over all other orders (meaning that it decays more slowly), while in the charge density wave (CDW) + spin density wave (SDW) phase both the density-density and spin-spin correlations are comparable. The AFM phase is evidenced by a strong spin-spin correlation peaked at momentum $k = \pi$, and the SC phase displays strong pairing correlations. These cases will be illustrated in detail in the next section.

III. RESULTS

The band structure and Fermi surface of the corresponding tight binding model are very sensitive to the sign of t_2 [54]:

$$\omega(k) = -2t_1 \cos(k) - 2t_2 \cos(2k).$$

We focus our study on two cases: (i) $t_2/t_1 = 0.5$ and (ii) $t_2/t_1 = -0.5$. For these values the system can realize four Fermi points, depending on the position of the Fermi level (or the density).

A. $t_2 = -0.5$

We start by first discussing the phase diagram for $t_2/t_1 = -0.5$, which is shown in Fig. 1. We obtain the ground-state energy for each particle number $N = 0, 1, \dots, L$ and use the Maxwell construction to find the chemical potential μ that minimizes the free energy $E_0 - \mu N$. This procedure is repeated for each value of J . The results for N vs μ are shown in Fig. 2. Different phases can be identified in this figure: When the system is in the (FM) metallic phase, N vs μ increases in steps of $\Delta N = 1$; phase segregation is evidenced by a discontinuity in N as a function of μ . For intermediate values of $J \sim t$, we observe jumps in steps of $\Delta N = 2$ that can be interpreted as possible evidence of pairing and a SC phase, although it could also be a finite-size effect. Compared to the conventional t - J model [55], the phase separation boundary in the t_1 - t_2 - J model is shifted to a larger J in the low-density area and to a smaller J in the high-density area (Fig. 1).

Phase separation is mostly a result of the strong tendency to AFM with increasing J . For sufficiently large J , spins prefer to be antiferromagnetically aligned and forming a domain of localized, strongly bound electrons, separated from a metallic ‘‘bubble.’’ On light doping, we can see in Fig. 9 that the negative t_2 favors antiferromagnetic order ($S(k)$ peaks at π) near half filling. However, in the conventional t - J model $S(k)$ is peaked at $2k_F$, so in the model with negative t_2 phase separation occurs earlier, with a smaller J . In the dilute limit, phase segregation is between AFM and PDW phases. The

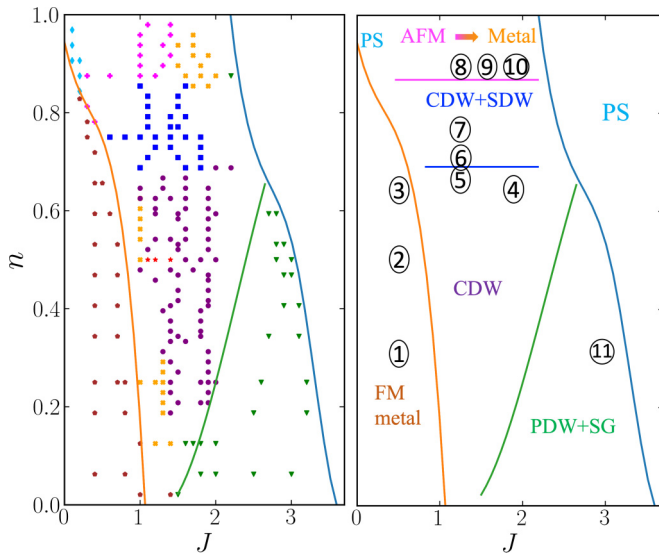


FIG. 1. Phase diagrams of the t_1 - t_2 - J model with $t_2 = -0.5$. Left: Phase diagram with markers representing each phase where correlations have been calculated. Right: Schematic phase diagram with each phase indicated by the label. FM: ferromagnetic; CDW: charge density wave; SDW: spin density wave; AFM: antiferromagnetic; PDW: pair density wave; SG: spin gapped; and PS: phase separation. The numbered circles indicate representative points used in the study. The brown pentagon, purple circle, blue square, and green triangle symbols on the left panel represent the data points corresponding to the FM metal, CDW, CDW+SDW, and PDW+SG, respectively; the yellow \times , pink plus, red star, and sky-blue diamond denote metal, AFM, SDW, and PS, respectively.

fact that pairing survives to larger J may be interpreted as evidence that in this regime the physics is dominated by the kinetic energy; electrons are farther apart in the t_1 - t_2 - J model than in the conventional t - J model. Because of the presence of the extra term with t_2 , the kinetic energy is larger (in absolute value) and a larger J is needed to destabilize this state.

By reading off the kinks on the N vs μ curves from the Maxwell construction, we can determine the critical values of the phase transitions. The kinks in the high-density region for $J = 0.1$ and $J = 0.5$ represent the FM metal phase boundary. We also notice a kink at $n = 0.5$ in these two curves. This point is not a phase boundary but a sort of ‘‘Lifshitz transition,’’ where the number of Fermi points in the momentum distribution changes from 4 to 2. Another feature that is worth noticing is the plateau at $n = 2/3$ when $J = 1.3, 1.7,$ and 2.1 . The position of this plateau is roughly on the line separating the CDW and CDW+SDW phases in Fig. 1. At this particular particle filling the charge correlations oscillate with period 3. Similarly, a CDW appears at quarter filling, where the charge order has period 4. However, at quarter filling the spin density wave is strong compared to the charge order, while at $n = 2/3$ the charge order is dominant, as we deduce from the correlations.

For small J , the (negative) second-neighbor hopping t_2 becomes the dominant perturbation by introducing frustrations: When J is not strong enough to induce antiferromagnetism, the ground state is a fully polarized ferromagnet. In order to investigate the dominant orders in this phase, we study

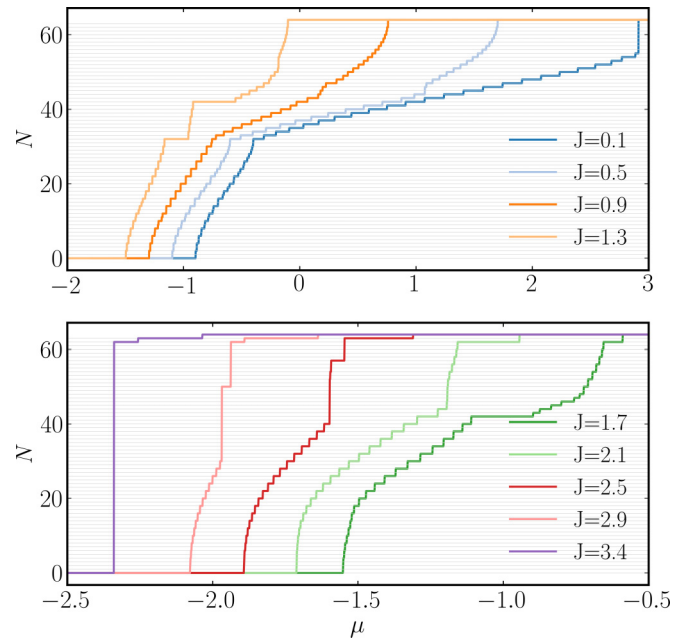


FIG. 2. Particle density as a function of the chemical potential for different values of J , obtained by means of a Maxwell construction. The value of J decreases from left to right.

the decaying behavior of the correlations. Our results suggest strong triplet-superconducting correlations in the FM metal. Depending on the doping concentration, three different types of the pairing order emerge in this phase [56–61]. In Fig. 3 we observe that the triplet pair-pair correlations exhibit a quasi-long-range oscillating SC order in the lower-density regime (Fig. 3(a)) but quasi-long-range PDW order at intermediate densities (Fig. 3(b)), where the pair-pair correlations oscillate around zero with vanishing spacial average. Eventually the uniform SC order is stabilized at higher density (Fig. 3(c)). We notice that PDW order has been proposed as a precursor to superconductivity but has only been observed in a handful of microscopic models [62–70], and the triplet PDW is even rarer [71]. Interestingly, we find there is a small region of phase separation in the high density area when J is very small (less than 0.3); this is evidenced by the jump in the N vs μ plot in Fig. 2. This means that the transition from the AFM phase to the Nagaoka FM phase is abrupt and requires a finite critical hole density. According to Nagaoka’s theorem, this density should approach zero as $J \rightarrow 0$ (or $U \rightarrow \infty$ in the Hubbard model), which is precisely what we see in Fig. 2.

Moving to larger J , away from the FM metal phase, we encounter a very rich region with many competing phases. At low particle density, several correlations have quasi-long-range order with similar power-law behavior, and we conclude that the system is in a metallic phase without a dominant instability, which could be also due to the bottom of the noninteracting dispersion becoming very flat in the presence of negative t_2 . By increasing the particle concentration, the system enters a CDW phase with dominant charge order, a subdominant pairing order, and gapped spin sector. As shown in Fig. 4, the density-density correlation fluctuates around

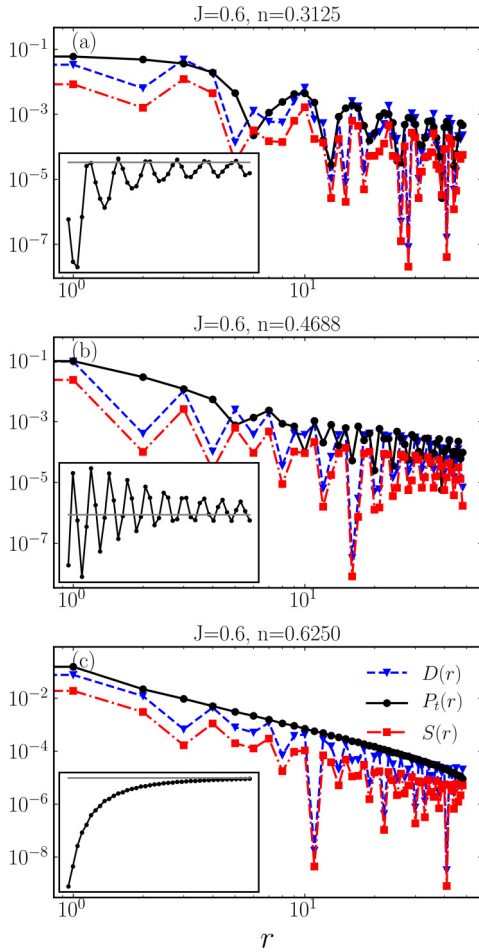


FIG. 3. Spin-spin, charge-charge, and triplet SC correlations in log-log scale for $t_2 = -0.5$ and $S_z = N_{\text{particle}}/2$. The parameter sets in panels (a), (b), and (c) are marked as ①, ②, and ③ in the phase diagram in Fig. 1. The insets show the raw data of triplet pairing correlations in real space. These results correspond to chains of length $L = 64$.

its average value (Fig. 4(b)), and we find sharp peaks in the density structure factor at $k = 2k_F$ (Fig. 4(c)). In addition, the local density profile displays large oscillations, unlikely to be due to Friedel oscillations or a boundary effect (Fig. 4(d)). As the density increases further, we observe changes in both the charge and spin sectors. When the system is in the CDW phase, the density structure factor $D(k)$ has an extra bump besides the dominant peak (red curve in Fig. 5(c)), and this anomaly in $D(k)$ eventually disappears as shown in Fig. 5(c). This subtle change in the charge order can also be observed in the local density profile (Fig. 5(b)), with multiple modes contributing to the oscillating pattern. However, as the density increases, only dominant mode survives. Meanwhile, the spin-spin correlation keeps getting enhanced (Fig. 5(d)). At the transition point where the SDW emerges, there is a plateau in the N vs μ curves (Fig. 2), which is an indication of a charge-gapped phase. As we approach half filling, AFM order eventually becomes dominant (Fig. 6(a)) and the spin structure factor peaks at π (Fig. 6(c)). However, this AFM phase evolves into a metallic phase (Fig. 6(b)) without a leading order when increasing J . The emergence

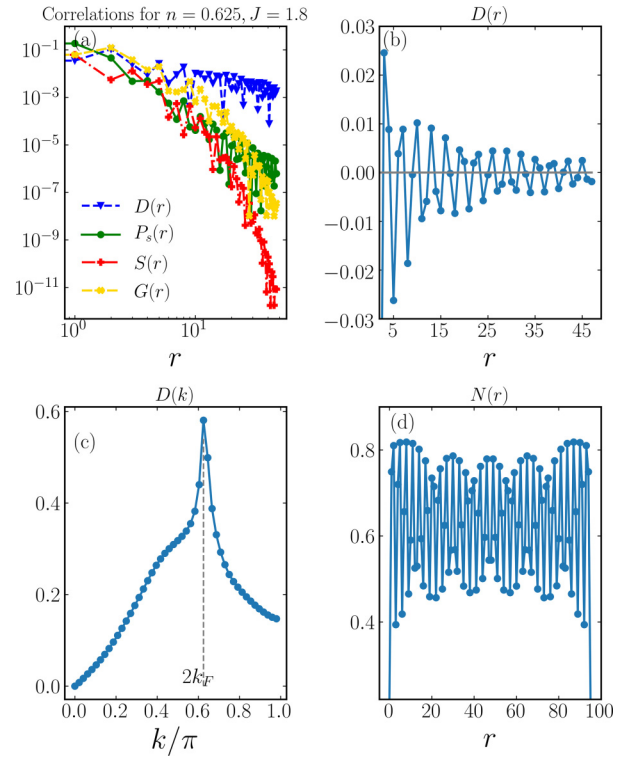


FIG. 4. Correlation functions for a t_1 - t_2 - J chain of length $L = 96$, density $n = 0.625$, $t_2 = -0.5$, and $J = 1.8$, corresponding to the point marked as ④ in the phase diagram, Fig. 1.

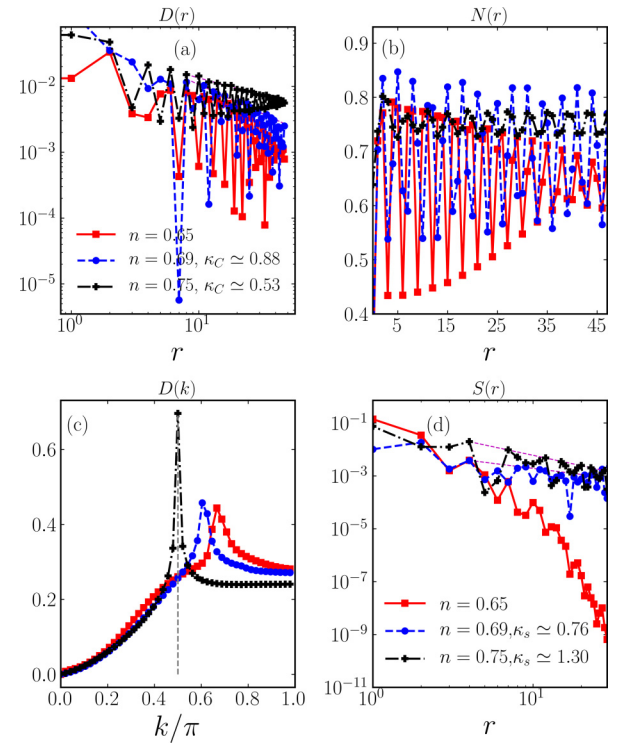


FIG. 5. Correlations for a t_1 - t_2 - J chain of length $L = 96$, $J = 1.3$, and $t_2 = -0.5$. The different densities n correspond to the points marked as ⑤, ⑥, and ⑦ in the phase diagram in Fig. 1. κ_C and κ_S represent the power-law decaying exponent of charge and spin orders, respectively. The thin dashed purple line corresponds to the curve fitting with respective κ value.

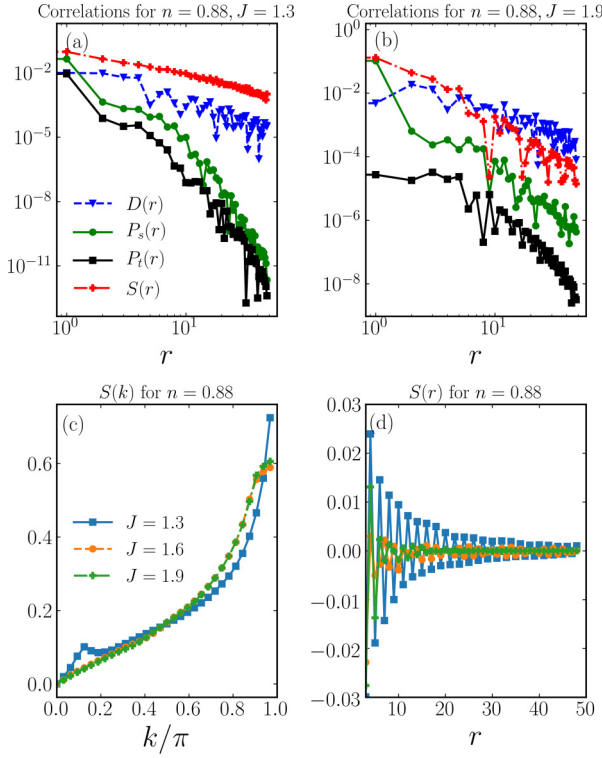


FIG. 6. Correlations for a t_1 - t_2 - J chain with $L = 64$, $n = N/L = 0.875$, and $t_2 = -0.5$. The values of J correspond to the points marked as $\textcircled{8}$, $\textcircled{9}$, and $\textcircled{10}$ in the phase diagram in Fig. 1.

of this metallic phase could be due to frustration since the AFM order is incompatible with the instabilities at the Fermi level.

Finally, at low particle density and large J , we encounter a singlet pair density wave before entering the phase separation region. This phase has dominant PDW quasi-long-range order, as shown in Fig. 7, which has a periodic oscillation in real

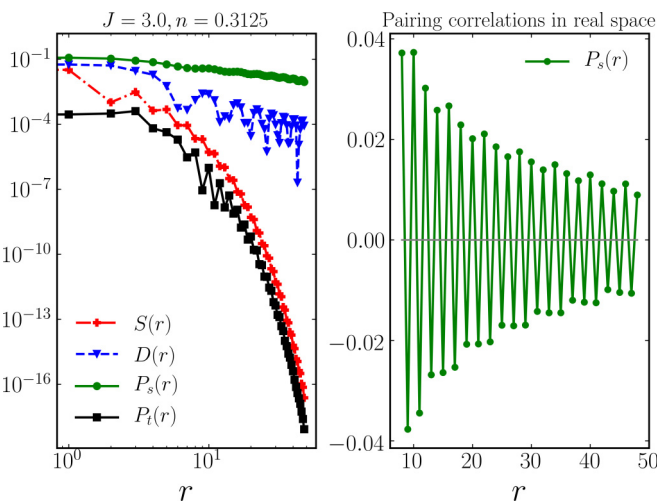


FIG. 7. Left: Spin-spin, charge-charge, singlet, and triplet pair-pair correlations in log-log scale. Right: Singlet pairing correlation in real space. The results are for $t_2 = -0.5$ corresponding to the points marked as $\textcircled{11}$ in the phase diagram in Fig. 1.

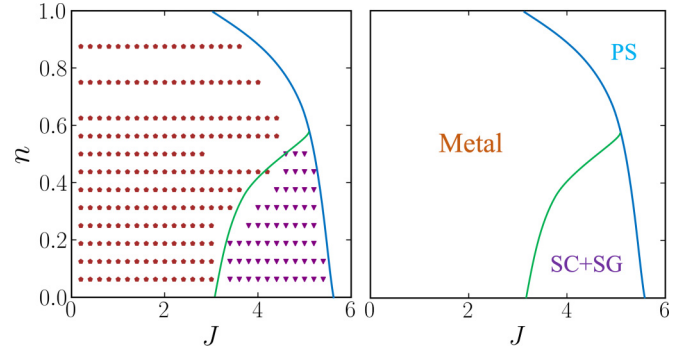


FIG. 8. Phase diagrams of t_1 - t_2 - J model with $t_2 = 0.5$. Left: Phase diagram with markers representing each phase. Right: Schematic phase diagram with each phase indicated by the label. SC: superconducting; SG: spin gapped; and PS: phase separation. The brown pentagon and purple triangle symbols on the left panel represent the data points corresponding to the metal and SC+SG, respectively.

space and vanishing spatial average. The boundary between the CDW and PDW phase is not well defined and resembles a crossover, with a narrow window where both order parameters decay with similar power-law exponent. In Fig. 2, we can see this paired phase displays jumps in the density in steps of 2 as a result of binding. In other words, states with odd number of electrons are not energetically stable due to pairing.

B. $t_2 = 0.5$

By means of a particle-hole transformation, the hole-doped t_1 - t_2 - J model with positive t_2/t_1 can be interpreted as the electron-doped side of the Mott insulator.

By conducting the similar computation as in Sec. III A, we have obtained the phase diagram for $t_2 = -0.5$, which is shown in Fig. 8. For a large region in this phase diagram the system exhibits a metallic phase; by increasing J it enters a

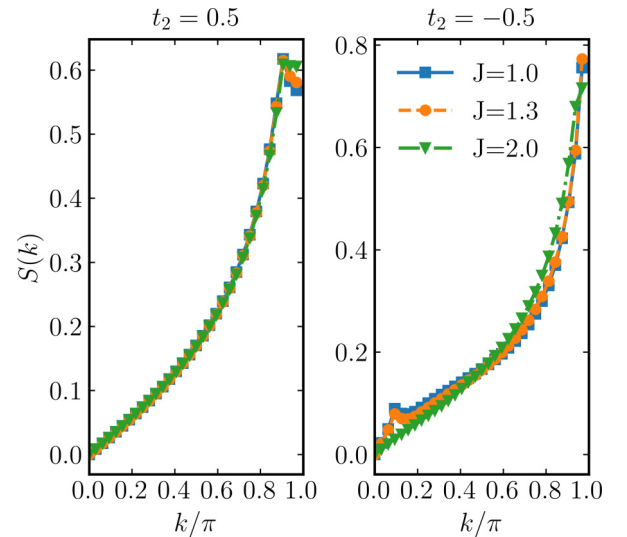


FIG. 9. Spin structure factor comparing the cases with $t_2 = 0.5$ and $t_2 = -0.5$. Results are for a chain with length $L = 64$ and fixed particle number $N = 58$.

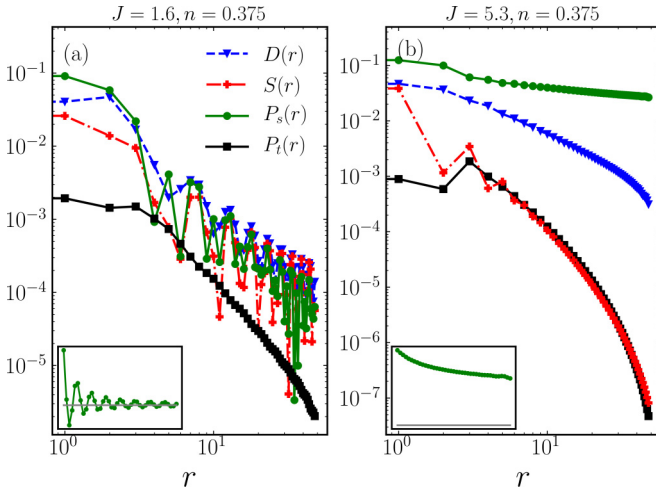


FIG. 10. Real space spin-spin, charge-charge, and singlet and triplet pair-pair correlations in log-log scale for $t_2 = 0.5$. The insets show the raw data of spatial singlet pair-pair correlations, where the gray lines mark the zero value.

spin-gapped superconducting region in the low-density area, and, finally, when J is large the system phase separates.

While negative t_2/t_1 changes the noninteracting Fermi surface at low densities, the physics of the positive t_2/t_1 case qualitatively resembles that of the conventional t - J model. The influence of the second-neighbor hopping on the Fermi surface becomes more dominant near half filling where the noninteracting band develops two local “maxima” away from $k = \pm\pi$.

The effects of the sign of t_2 on magnetism can be observed in the spin structure factors: Instead of the stable AFM π peak observed on the hole-doped side, the spin structure factor now peaks at $2k_F$, which means that upon doping, the system exhibits a SDW instead of Néel-like AFM order (Fig. 9), and all the correlations have similar scaling behavior. In the metallic phase we do not encounter a dominant instability. However, we find that the superconducting order parameter oscillates in space, consistent with a PDW (inset of Fig. 10(a)) coexisting with spin and charge orders, and all correlations with comparable scaling behavior.

Similarly to the original t - J model, a spin-gapped SC phase emerges in the low-density region with large J (Fig. 10(b)) as an intermediate phase before the system phase separates. Unlike the Luther-Emery phase discovered in the t - J model [55], the SC phase is not accompanied by a charge order.

IV. CONCLUSIONS

We present a systematic study of the phase diagrams of the t - J model with second-neighbor hopping using the DMRG method. This model provides a simple and rich testbed to investigate the interplay among kinetic frustration, magnetism, and superconductivity. In addition, by applying a particle-hole transformation, it yields information about the physics

of hole-doped and particle-doped antiferromagnets. By tuning the interaction J and filling factor n , as well as the sign of t_2 , we obtained complex phase diagrams.

When t_2/t_1 is negative (-0.5), the system is AFM at half-filling but becomes fully spin polarized upon doping in the strongly interacting limit (small J). This FM metal phase is also accompanied by a quasi-long-range triplet superconductivity order. In the single-particle picture, there are four Fermi points below quarter filling. As a consequence, magnetic order is frustrated and a CDW phase emerges. The CDW order becomes intertwined with a SDW order at larger particle density. By further increasing J , they yield to a singlet-SC phase with subdominant charge order and a spin gap.

When t_2/t_1 is positive (0.5), the phase diagram of the t_1 - t_2 - J model qualitatively resembles that of the conventional t - J model. The system realizes a large metallic phase at all densities when J is smaller than the bandwidth, with all sectors gapless. By increasing J , the pair correlations become more dominant. Eventually, a spin-gapped superconducting phase develops in the low-density regime.

It would be interesting to find analogs of the observed phases in the phase diagram of the cuprate superconductors [1–7]. The one-dimensional t_1 - t_2 - J model shares some similarities with the two-dimensional materials, such as many competing instabilities on the hole-doped side ($t_2 < 0$), and a SDW in the intermediate region between the AFM and superconducting domains upon doping. In contrast, some of the observed features are inconsistent with the phases observed in high- T_c superconducting materials: In 2D cuprates, the AFM domain is more robust on the electron-doped side, however, for the 1D model, the AFM order is fragile and quickly being replaced by an SDW instability upon electron doping. This discrepancy between 1D and 2D may stem primarily from the different definitions of the “second-neighbor hopping,” which in a 2D lattice corresponds to hopping across square plaquettes. Finally, we point out that singlet and triplet PDW may be more common than usually recognized. Evidence in our work point to the presence of multiple Fermi points as the culprits. Even though these phases have short-range correlations in our model, it would be interesting to understand the fundamental ingredients to stabilize them in higher dimensions.

ACKNOWLEDGMENTS

L.Y. acknowledges the support from the Department of Energy, Office of Science, Basic Energy Sciences, Materials Sciences and Engineering Division, under Contract No. DE-AC02-76SF00515. A.E.F. is supported by the National Science Foundation under Grant No. DMR-2120501. We acknowledge generous computational resources provided by Northeastern University’s Discovery Cluster at the Massachusetts Green High Performance Computing Center (MGHPCC) and the Sherlock cluster at Stanford University. Parts of the calculations are performed using the ITensor library [72,73].

- [1] B. Keimer, S. A. Kivelson, M. R. Norman, S. Uchida, and J. Zaanen, From quantum matter to high-temperature superconductivity in copper oxides, *Nature (London)* **518**, 179 (2015).
- [2] N. P. Armitage, P. Fournier, and R. L. Greene, Progress and perspectives on electron-doped cuprates, *Rev. Mod. Phys.* **82**, 2421 (2010).
- [3] D. Rybicki, M. Jurkutat, S. Reichardt, C. Kapusta, and J. Haase, Perspective on the phase diagram of cuprate high-temperature superconductors, *Nat. Commun.* **7**, 11413 (2016).
- [4] S. Sachdev, M. A. Metlitski, Y. Qi, and C. Xu, Fluctuating spin density waves in metals, *Phys. Rev. B* **80**, 155129 (2009).
- [5] A. Damascelli, Z. Hussain, and Z.-X. Shen, Angle-resolved photoemission studies of the cuprate superconductors, *Rev. Mod. Phys.* **75**, 473 (2003).
- [6] P. A. Lee, N. Nagaosa, and X.-G. Wen, Doping a Mott insulator: Physics of high-temperature superconductivity, *Rev. Mod. Phys.* **78**, 17 (2006).
- [7] J. A. Sobota, Y. He, and Z.-X. Shen, Angle-resolved photoemission studies of quantum materials, *Rev. Mod. Phys.* **93**, 025006 (2021).
- [8] M. S. Hybertsen, E. B. Stechel, M. Schluter, and D. R. Jennison, Renormalization from density-functional theory to strong-coupling models for electronic states in Cu-O materials, *Phys. Rev. B* **41**, 11068 (1990).
- [9] S. B. Bacci, E. R. Gagliano, R. M. Martin, and J. F. Annett, Derivation of a one-band Hubbard model for CuO planar materials, *Phys. Rev. B* **44**, 7504 (1991).
- [10] T. Tohyama and S. Maekawa, Role of next-nearest-neighbor hopping in the $t-t'-J$ model, *Phys. Rev. B* **49**, 3596 (1994).
- [11] C. J. Calzado and J.-P. Malrieu, Proposal of an extended $t-J$ Hamiltonian for high- T_c cuprates from *ab initio* calculations on embedded clusters, *Phys. Rev. B* **63**, 214520 (2001).
- [12] G. I. Japaridze, R. M. Noack, D. Baeriswyl, and L. Tincani, Phases and phase transitions in the half-filled $t-t'$ Hubbard chain, *Phys. Rev. B* **76**, 115118 (2007).
- [13] H. Eskes, G. Sawatzky, and L. Feiner, Effective transfer for singlets formed by hole doping in the high- T_c superconductors, *Physica C: Superconduct.* **160**, 424 (1989).
- [14] H. Eskes and G. A. Sawatzky, Single-, triple-, or multiple-band Hubbard models, *Phys. Rev. B* **44**, 9656 (1991).
- [15] H. Eskes and G. A. Sawatzky, Doping dependence of high-energy spectral weights for the high- T_c cuprates, *Phys. Rev. B* **43**, 119 (1991).
- [16] D. Scalapino, Numerical studies of the 2d Hubbard model, in *Handbook of High-Temperature Superconductivity*, edited by J. R. Schrieffer and J. S. Brooks (Springer, New York, 2007), pp. 495–526.
- [17] B. Ponsioen, S. S. Chung, and P. Corboz, Period 4 stripe in the extended two-dimensional Hubbard model, *Phys. Rev. B* **100**, 195141 (2019).
- [18] M. Qin, T. Schäfer, S. Andergassen, P. Corboz, and E. Gull, The Hubbard model: A computational perspective, *Annu. Rev. Condens. Matter Phys.* **13**, 275 (2022).
- [19] S. Jiang, D. J. Scalapino, and S. R. White, Ground state phase diagram of the $t-t'-J$ Model, *Proc. Natl. Acad. Sci. USA* **118**, e2109978118 (2021).
- [20] S. Gong, W. Zhu, and D. N. Sheng, Robust d -wave superconductivity in the square-lattice $t - J$ model, *Phys. Rev. Lett.* **127**, 097003 (2021).
- [21] X. Lu, F. Chen, W. Zhu, D. N. Sheng, and S.-S. Gong, Emergent superconductivity and competing charge orders in hole-doped square-lattice $t - J$ model, *Phys. Rev. Lett.* **132**, 066002 (2024).
- [22] F. Chen, F. D. M. Haldane, and D. N. Sheng, D -wave and pair-density-wave superconductivity in the square-lattice $t - J$ model, [arXiv:2311.15092](https://arxiv.org/abs/2311.15092).
- [23] S. R. White and D. J. Scalapino, Competition between stripes and pairing in a $t - t' - J$ model, *Phys. Rev. B* **60**, R753 (1999).
- [24] M. Ogata, Stripe states in $t - t' - J$ model from a variational viewpoint, *Physica C: Superconduct.* **481**, 125 (2012).
- [25] A. Himeda, T. Kato, and M. Ogata, Stripe states with spatially oscillating d -wave superconductivity in the two-dimensional $t - t' - J$ model, *Phys. Rev. Lett.* **88**, 117001 (2002).
- [26] C. T. Shih, T. K. Lee, R. Eder, C.-Y. Mou, and Y. C. Chen, Enhancement of pairing correlation by t' in the two-dimensional extended $t - J$ model, *Phys. Rev. Lett.* **92**, 227002 (2004).
- [27] H.-C. Jiang, Z.-Y. Weng, and S. A. Kivelson, Superconductivity in the doped $t - J$ model: Results for four-leg cylinders, *Phys. Rev. B* **98**, 140505(R) (2018).
- [28] H.-C. Jiang and T. P. Devereaux, Superconductivity in the doped Hubbard model and its interplay with next-nearest hopping t' , *Science* **365**, 1424 (2019).
- [29] Y.-F. Jiang, J. Zaanen, T. P. Devereaux, and H.-C. Jiang, Ground state phase diagram of the doped Hubbard model on the four-leg cylinder, *Phys. Rev. Res.* **2**, 033073 (2020).
- [30] E. W. Huang, C. B. Mendl, S. Liu, S. Johnston, H.-C. Jiang, B. Moritz, and T. P. Devereaux, Numerical evidence of fluctuating stripes in the normal state of high- T_c cuprate superconductors, *Science* **358**, 1161 (2017).
- [31] E. W. Huang, C. B. Mendl, H.-C. Jiang, B. Moritz, and T. P. Devereaux, Stripe order from the perspective of the Hubbard model, *npj Quant. Mater.* **3**, 22 (2018).
- [32] O. Zachar, Staggered liquid phases of the one-dimensional Kondo-Heisenberg lattice model, *Phys. Rev. B* **63**, 205104 (2001).
- [33] E. Fradkin, S. A. Kivelson, and J. M. Tranquada, Colloquium: Theory of intertwined orders in high temperature superconductors, *Rev. Mod. Phys.* **87**, 457 (2015).
- [34] H. Mukuda, S. Shimizu, A. Iyo, and Y. Kitaoka, High- T_c superconductivity and antiferromagnetism in multilayered copper oxides—A new paradigm of superconducting mechanism—, *J. Phys. Soc. Jpn.* **81**, 011008 (2012).
- [35] Z. Chen, Y. Wang, S. N. Rebec, T. Jia, M. Hashimoto, D. Lu, B. Moritz, R. G. Moore, T. P. Devereaux, and Z.-X. Shen, Anomalous strong near-neighbor attraction in doped 1D cuprate chains, *Science* **373**, 1235 (2021).
- [36] A. E. Feiguin, C. Helman, and A. A. Aligia, Effective one-band models for the one-dimensional cuprate $\text{Ba}_{2-x}\text{Sr}_x\text{CuO}_{3+\delta}$, *Phys. Rev. B* **108**, 075125 (2023).
- [37] U. Kumar, A. Nocera, G. Price, K. Stiwwinter, S. Johnston, and T. Datta, Spectroscopic signatures of next-nearest-neighbor hopping in the charge and spin dynamics of doped one-dimensional antiferromagnets, *Phys. Rev. B* **102**, 075134 (2020).
- [38] R. Eder and Y. Ohta, One-dimensional $t - J$ model with next-nearest-neighbor hopping: Breakdown of the Luttinger liquid, *Phys. Rev. B* **56**, R14247 (1997).
- [39] K. Sano and K. Takano, Bound state of a hole and a triplet spin in the $t_1 - t_2 - J_1 - J_2$ model, *Phys. Rev. B* **83**, 054421 (2011).

- [40] S. Onari, R. Arita, K. Kuroki, and H. Aoki, Spin-triplet superconductivity induced by charge fluctuations in extended Hubbard model, *J. Phys. Soc. Jpn.* **74**, 2579 (2005).
- [41] G. Carleo, S. Moroni, F. Becca, and S. Baroni, Itinerant ferromagnetic phase of the Hubbard model, *Phys. Rev. B* **83**, 060411(R) (2011).
- [42] L. Liu, H. Yao, E. Berg, S. R. White, and S. A. Kivelson, Phases of the infinite u Hubbard model on square lattices, *Phys. Rev. Lett.* **108**, 126406 (2012).
- [43] S. Milner, P. Weinberg, and A. Feiguin, Ferromagnetism and doublon localization in a Wannier-Hubbard chain, *Phys. Rev. B* **106**, 035128 (2022).
- [44] Y. Nagaoka, Ferromagnetism in a narrow, almost half-filled s band, *Phys. Rev.* **147**, 392 (1966).
- [45] D. C. Mattis and R. E. Peña, Effect of band structure on ferromagnetism, *Phys. Rev. B* **10**, 1006 (1974).
- [46] S. Daul and R. M. Noack, Ferromagnetic transition and phase diagram of the one-dimensional Hubbard model with next-nearest-neighbor hopping, *Phys. Rev. B* **58**, 2635 (1998).
- [47] E. Müller-Hartmann, Ferromagnetism in Hubbard models: Low density route, *J. Low Temp. Phys.* **99**, 349 (1995).
- [48] R. Hlubina, Phase diagram of the weak-coupling two-dimensional $t - t'$ Hubbard model at low and intermediate electron density, *Phys. Rev. B* **59**, 9600 (1999).
- [49] M. S. Anwar, S. R. Lee, R. Ishiguro, Y. Sugimoto, Y. Tano, S. J. Kang, Y. J. Shin, S. Yonezawa, D. Manske, H. Takayanagi, T. W. Noh, and Y. Maeno, Direct penetration of spin-triplet superconductivity into a ferromagnet in Au/SrRuO₃/Sr₂RuO₄ junctions, *Nat. Commun.* **7**, 13220 (2016).
- [50] S. Ran, C. Eckberg, Q.-P. Ding, Y. Furukawa, T. Metz, S. R. Saha, I.-L. Liu, M. Zic, H. Kim, J. Paglione, and N. P. Butch, Nearly ferromagnetic spin-triplet superconductivity, *Science* **365**, 684 (2019).
- [51] G. I. Japaridze and E. Müller-Hartmann, Triplet superconductivity in a one-dimensional ferromagnetic $t - J$ model, *Phys. Rev. B* **61**, 9019 (2000).
- [52] S. R. White, Density matrix formulation for quantum renormalization groups, *Phys. Rev. Lett.* **69**, 2863 (1992).
- [53] S. R. White, Density-matrix algorithms for quantum renormalization groups, *Phys. Rev. B* **48**, 10345 (1993).
- [54] G. B. Martins, J. C. Xavier, L. Arrachea, and E. Dagotto, Qualitative understanding of the sign of t' asymmetry in the extended $t - J$ model and relevance for pairing properties, *Phys. Rev. B* **64**, 180513(R) (2001).
- [55] A. Moreno, A. Muramatsu, and S. R. Manmana, Ground-state phase diagram of the one-dimensional $t - J$ model, *Phys. Rev. B* **83**, 205113 (2011).
- [56] J. Bardeen, L. N. Cooper, and J. R. Schrieffer, Theory of superconductivity, *Phys. Rev.* **108**, 1175 (1957).
- [57] P. Fulde and R. A. Ferrell, Superconductivity in a strong spin-exchange field, *Phys. Rev.* **135**, A550 (1964).
- [58] A. I. Larkin and Y. N. Ovchinnikov, Nonuniform state of superconductors, *Sov. Phys. J. Exp. Theor. Phys.* **20**, 762 (1965).
- [59] D. F. Agterberg, J. S. Davis, S. D. Edkins, E. Fradkin, D. J. Van Harlingen, S. A. Kivelson, P. A. Lee, L. Radzihovsky, J. M. Tranquada, and Y. Wang, The physics of pair-density waves: Cuprate superconductors and beyond, *Annu. Rev. Condens. Matter Phys.* **11**, 231 (2020).
- [60] A. E. Feiguin and M. P. A. Fisher, Exotic paired states with anisotropic spin-dependent fermi surfaces, *Phys. Rev. Lett.* **103**, 025303 (2009).
- [61] A. E. Feiguin and M. P. A. Fisher, Exotic paired phases in ladders with spin-dependent hopping, *Phys. Rev. B* **83**, 115104 (2011).
- [62] E. Berg, E. Fradkin, and S. A. Kivelson, Pair-density-wave correlations in the Kondo-Heisenberg model, *Phys. Rev. Lett.* **105**, 146403 (2010).
- [63] J. Almeida, G. Roux, and D. Poilblanc, Pair density waves in coupled doped two-leg ladders, *Phys. Rev. B* **82**, 041102(R) (2010).
- [64] A. Jaefari and E. Fradkin, Pair-density-wave superconducting order in two-leg ladders, *Phys. Rev. B* **85**, 035104 (2012).
- [65] M. Zegrodnik and J. Spałek, Incorporation of charge- and pair-density-wave states into the one-band model of d -wave superconductivity, *Phys. Rev. B* **98**, 155144 (2018).
- [66] X. Y. Xu, K. T. Law, and P. A. Lee, Pair density wave in the doped $t - j$ model with ring exchange on a triangular lattice, *Phys. Rev. Lett.* **122**, 167001 (2019).
- [67] J. May-Mann, R. Levy, R. Soto-Garrido, G. Y. Cho, B. K. Clark, and E. Fradkin, Topology and the one-dimensional Kondo-Heisenberg model, *Phys. Rev. B* **101**, 165133 (2020).
- [68] Y.-H. Zhang and A. Vishwanath, Pair-density-wave superconductor from doping Haldane chain and rung-singlet ladder, *Phys. Rev. B* **106**, 045103 (2022).
- [69] H.-C. Jiang, Pair density wave in the doped three-band Hubbard model on two-leg square cylinders, *Phys. Rev. B* **107**, 214504 (2023).
- [70] L. Yang, T. P. Devereaux, and H.-C. Jiang, Recovery of a luther-emery phase in the three-band Hubbard model with longer-range hopping, [arXiv:2310.17706](https://arxiv.org/abs/2310.17706).
- [71] D. Shaffer and L. H. Santos, Triplet pair density wave superconductivity on the π -flux square lattice, *Phys. Rev. B* **108**, 035135 (2023).
- [72] M. Fishman, S. R. White, and E. M. Stoudenmire, The ITensor software library for tensor network calculations, *SciPost Phys. Codebases*, 4 (2022).
- [73] M. Fishman, S. R. White, and E. M. Stoudenmire, Codebase release 0.3 for ITensor, *SciPost Phys. Codebases*, 4-r0.3 (2022).

Correction: The Grant number in the Acknowledgment section contained an error and has been fixed.